bioRxiv preprint doi: https://doi.org/10.1101/745745; this version posted August 24, 2019. The copyright holder for this preprint (which was not certified by peer review) is the author/funder, who has granted bioRxiv a license to display the preprint in perpetuity. It is made available under aCC-BY-NC 4.0 International license.

Phase-based coordination of hippocampal and neocortical oscillations during human sleep

Roy Cox[1*], Theodor Rüber[1,2,3], Bernhard P Staresina[4], Juergen Fell[1]

1: Department of Epileptology, University of Bonn, 53127 Bonn, Germany
2: Epilepsy Center Frankfurt Rhine-Main, Department of Neurology, Goethe University Frankfurt, 60590 Frankfurt am Main, Germany
3: Center for Personalized Translational Epilepsy Research (CePTER), Goethe University Frankfurt, 60590 Frankfurt am Main, Germany
4: School of Psychology, University of Birmingham, B15 2TT Birmingham, United Kingdom

* corresponding author: roycox.roycox@gmail.com

Abstract

During sleep, new memories undergo a gradual transfer from the hippocampus (HPC) to the neocortex (NC). Precisely timed neural oscillations interacting within and between these brain structures are thought to mediate this sleep-dependent memory consolidation. Although slow oscillations (SOs), sleep spindles, and ripples have received the most attention, exactly which sleep oscillations instantiate the HPC-NC dialog, and via what mechanisms, remains elusive. Employing invasive electroencephalography in 10 neurosurgical patients across a full night of sleep, we identified three broad classes of phase-based HPC-NC communication. First, we observed interregional phase synchrony for non-rapid eye movement (NREM) spindles, N2 and rapid eye movement (REM) theta, and N3 beta activity. Second, we found asymmetrical N3 cross-frequency coupling between HPC SOs and NC activity spanning the delta to ripple bands, but not for the opposite direction. Lastly, NREM theta and spindle synchrony were themselves modulated by HPC SOs. These novel forms of phase-based interregional communication emphasize the role of HPC SOs in the HPC-NC dialog, and may offer a physiological basis for the sleep-dependent reorganization of mnemonic content.

bioRxiv preprint doi: https://doi.org/10.1101/745745; this version posted August 24, 2019. The copyright holder for this preprint (which was not certified by peer review) is the author/funder, who has granted bioRxiv a license to display the preprint in perpetuity. It is made available under aCC-BY-NC 4.0 International license.

Introduction

A long-standing question in cognitive neuroscience asks how initially fragile episodic memories are transformed into lasting representations. Theoretical accounts postulate that this process involves a protracted transfer of memories from the hippocampus (HPC) to neocortical (NC) domains (1–3), with a large body of lesion (4, 5), and neuroimaging (6, 7) findings supporting this notion. One NC area of particular interest is the lateral temporal cortex, a convergence zone involved in long-term memory storage (8, 9), representing higher order visual, categorical, and semantic concepts (10–12).

Intriguingly, sleep leads to more stable and better integrated episodic memories (13, 14), suggesting a pivotal role for this brain state in the systems-level reorganization of memory traces (15). Neural oscillations, especially non-rapid eye movement (NREM) neocortical slow oscillations (SOs; 0.5-1 Hz), thalamocortical sleep spindles (12-16 Hz), and hippocampal ripples (80-100 Hz), are widely held to mediate the HPC-NC memory transfer and consolidation process (16–21), particularly given the presence of both SOs and spindles in HPC (22–25). Moreover, various other spectral components exist in electrophysiological recordings of human sleep, with recent evidence suggesting potential roles for theta (4–8 Hz) in NREM (26, 27) and rapid eye movement (REM) (28, 29) memory processing, complicating the question of which oscillatory rhythms instantiate the HPC-NC dialog.

A large body of evidence indicates that oscillatory phase has a critical influence on neuronal excitability and activity (30), thereby offering a precise temporal scaffold for orchestrating neural processing within and across brain structures (31, 32). As such, oscillatory phase coordination between HPC and NC is a prime candidate mechanism for sleep-dependent information exchange between these areas. However, various forms of phase coupling may be distinguished, and phase-based HPC-NC interactions during sleep could be implemented in at least three (non-mutually exclusive) ways.

First, consistent oscillatory phase locking between brain regions at the same frequency is thought to enable effective communication between the underlying neuronal groups (33). Phase synchrony during sleep has been reported between cortical regions for various frequency bands (34), including the spindle (35, 36) and gamma (37) ranges, and between HPC and prefrontal areas in the spindle range (38). Whether similar phenomena exist between human HPC and extrafrontal NC areas, for which frequency bands, and in which sleep stages, has not been examined.

Beside potential phase coupling *within* frequency bands, NREM sleep oscillations are also temporally organized *across* frequency bands. Such cross-frequency phase-amplitude coupling (PAC) is thought to enable brain communication across multiple spatiotemporal scales (39, 40). Local PAC among SOs, spindles, and ripples has been well characterized for various brain structures including HPC (24, 35, 41–46), and is considered a fundamental building block of memory consolidation theories (47). However, local PAC exists for other frequency pairs (48), with SOs exerting particularly powerful drives not only over spindle and ripple activity, but also over delta (49), theta (50), and gamma (35, 37) components. Extending the notion of local PAC to cross-regional interactions, the phase of a slower rhythm in one brain structure may modulate expression of faster activity at the other site (24, 46, 51), thus constituting a second potential form of HPC-NC communication.

bioRxiv preprint doi: https://doi.org/10.1101/745745; this version posted August 24, 2019. The copyright holder for this preprint (which was not certified by peer review) is the author/funder, who has granted bioRxiv a license to display the preprint in perpetuity. It is made available under aCC-BY-NC 4.0 International license.

Third, interregional phase synchronization within a frequency band might itself be modulated by the phase of a slower rhythm, as shown for the SO-phase-dependent coordination of spindle synchrony in cortical networks (35). Whether analogous SO-based modulation of phase synchronization exists between HPC and NC, and if so, for which frequency components, remains unexplored.

Here, we examined intracranial electrophysiological activity in a sample of 10 presurgical epilepsy patients during light NREM (N2), deep NREM (N3) and REM sleep. Specifically, we focused on HPC and lateral temporal cortex as a site relevant for long-term memory storage. We hypothesized that these areas exhibit interregional phase coordination, which could manifest in any or all of the three aforementioned forms of coupling. Given both the theoretical importance of nested SO-spindle-ripple activity (52), and inconclusive evidence regarding the directionality of HPC-NC coupling (22, 25, 38, 53–56), we were particularly interested in whether HPC and NC SOs or spindles modulate faster activity at the other brain site, and if so, whether these effects are direction-dependent. Moreover, we considered a wide 0.5–200 Hz frequency range to allow potential identification of oscillatory communication lines outside the SO-spindle-ripple framework. Using this approach, we identified several novel forms of phase-based HPC-NC communication centered on SO, spindle, theta, and beta activity, thereby offering a potential neurobiological substrate for sleep-dependent memory consolidation.

Results

We analyzed overnight invasive electroencephalography (EEG) from the hippocampus (HPC) and lateral temporal neocortex (NC) in a sample of 10 epilepsy patients during N2, N3 and REM sleep. Polysomnography-based sleep architecture was in line with healthy sleep (Supp. Table 1). Only intracranial contacts from the non-pathological hemisphere were used, as evidenced by clinical monitoring (Supp. Table 2).

Spindle, theta, and beta phase synchronization between hippocampus and neocortex

Following inspection of raw traces with spectrograms (Supp. Fig. 1), and power spectra (Supp. Fig 2), we evaluated whether, and to what degree, oscillatory signals in HPC and NC show phase coordination within frequency bands. Using the weighted phase lag index (wPLI: a metric minimally sensitive to common neural sources (57)), we observed that raw wPLI showed a general decrease with frequency (Fig. 1A), with slower rhythms showing stronger synchrony than fast oscillations, as typically observed (58). However, clear departures from this downward trend appeared for three main frequency bands. First, phase synchrony was enhanced in the spindle range (peak frequency: 13.6 Hz) during N2 and N3, consistent with findings from other brain sites (35, 38). Surprisingly, however, synchronization enhancements were also observed in the theta range (7.4 Hz) during N2 and REM, and in the beta range (28 Hz) during N3. These observations were supported by significant stage differences in the pertaining frequency bands (colored bars at top of Fig. 1A, cluster-based permutation tests, all $P<0.05$). Small but systematic stage differences were also found for frequency bins in the gamma range (75 and 122 Hz; N3>N2).

bioRxiv preprint doi: https://doi.org/10.1101/745745; this version posted August 24, 2019. The copyright holder for this preprint (which was not certified by peer review) is the author/funder, who has granted bioRxiv a license to display the preprint in perpetuity. It is made available under aCC-BY-NC 4.0 International license.

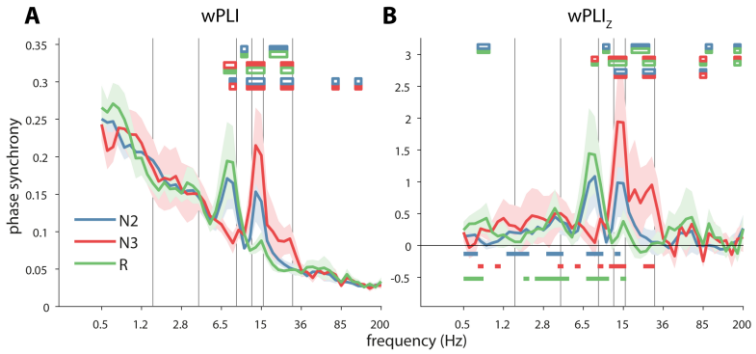

Figure 1. Phase synchrony between hippocampus and necortex. Group-level connectivity profiles for (unnormalized) wPLI (A) and (normalized) wPLI$_Z$ (B). Horizontal color bars at top of both panels indicate significant pairwise stage differences (two-tailed cluster-based permutation tests, P<0.05). Filled color reflects stage with greater connectivity. Horizontal color bars at bottom of panel (B) indicate above-chance connectivity one-tailed cluster-based permutation tests versus zero, P<0.05). Error shading: standard error of the mean across patients. Gray vertical lines at 1.5, 4, 9, 12.5, 16 and 30 Hz indicate approximate boundaries between SO, delta, theta, slow spindle, fast spindle, beta, and faster activity.

To determine whether phase coupling in these or any other frequency bands was beyond chance levels, we z-scored raw wPLI values with respect to time-shifted surrogate distributions. This procedure essentially removed the downward trend, while retaining the aforementioned theta, spindle, and beta peaks (Fig. 1B). Comparing wPLI$_Z$ values to zero (cluster-based permutation tests) indicated above-chance HPC-NC phase coordination in the theta range for N2 and REM (significant ranges indicated by colored bars at bottom of Fig. 1B). Significant spindle connectivity was seen for N3 and N2, and less prominently, REM, while beta connectivity occurred exclusively during N3. Importantly, each of these effects could also be discerned on an individual basis (Supp. Fig. 3ABC). Weaker group-level effects of above-zero coupling were observed in the SO and delta ranges, primarily during N2 and REM. Interestingly, only limited SO-based connectivity was seen during N3, suggesting that SO phase relations between HPC and NC are relatively variable (25, 38). No systematic effects emerged for frequencies beyond beta.

Sleep stage comparisons for the normalized wPLI$_Z$ metric were highly consistent with results using the raw metric, including theta-, spindle-, and beta-related effects (significant ranges indicated by colored bars at top of Fig. 1B). Moreover, SO-based coupling was found to be reliably greater during REM than N2, consistent with the notion that SOs may occur during REM (59). Finally, while small stage differences emerged at frequencies >70 Hz, none of these frequency bands showed above-chance coupling.

Finally, various control analyses showed that phase synchrony was not systematically related to power (Supp. Results). Overall, these findings indicate a precise phase-based coordination between HPC and NC rhythms, primarily in the spindle, theta, and beta ranges, thus signifying the existence of communication lines beyond the canonical NREM oscillators.

Cross-frequency coupling of neocortical activity to hippocampal slow oscillations

Next, we turned our attention to interactions between, rather than within, frequency bands. We quantified cross-frequency coupling using the debiased phase-amplitude coupling metric (dPAC: a metric correcting for potential non-sinusoidality of the phase-providing frequency (60)). These values were further z-scored with respect to surrogate distributions.

bioRxiv preprint doi: https://doi.org/10.1101/745745; this version posted August 24, 2019. The copyright holder for this preprint (which was not certified by peer review) is the author/funder, who has granted bioRxiv a license to display the preprint in perpetuity. It is made available under aCC-BY-NC 4.0 International license.

The resulting metric ($dPAC_Z$) signifies the degree to which activity at a faster frequency is non-uniformly distributed across the phase of a slower frequency.

Following analyses of local PAC within HPC and NC separately (Supp. Results and Supp. Fig. 4), we asked whether the oscillatory phase in one brain area could modulate faster activity in the other region. Assessing whether the phase of HPC rhythms coordinates faster activity in NC ("HPC-NC PAC"), we found that HPC SOs (0.5-1 Hz) robustly orchestrate the expression of faster activity in NC during N3 sleep (Fig. 2A). Specifically, distinct hotspots were found for modulated frequencies in the delta (maximum: 3.5 Hz), theta (6.5 Hz), spindle/beta (17 Hz), beta/gamma (32 Hz), and high-gamma/ripple (85 Hz) ranges (white arrows in Fig. 2A). A weak SO-ripple (85 Hz) cluster also emerged during N2. No systematic cross-regional modulation of neocortical activity by the hippocampal phase was observed during REM sleep.

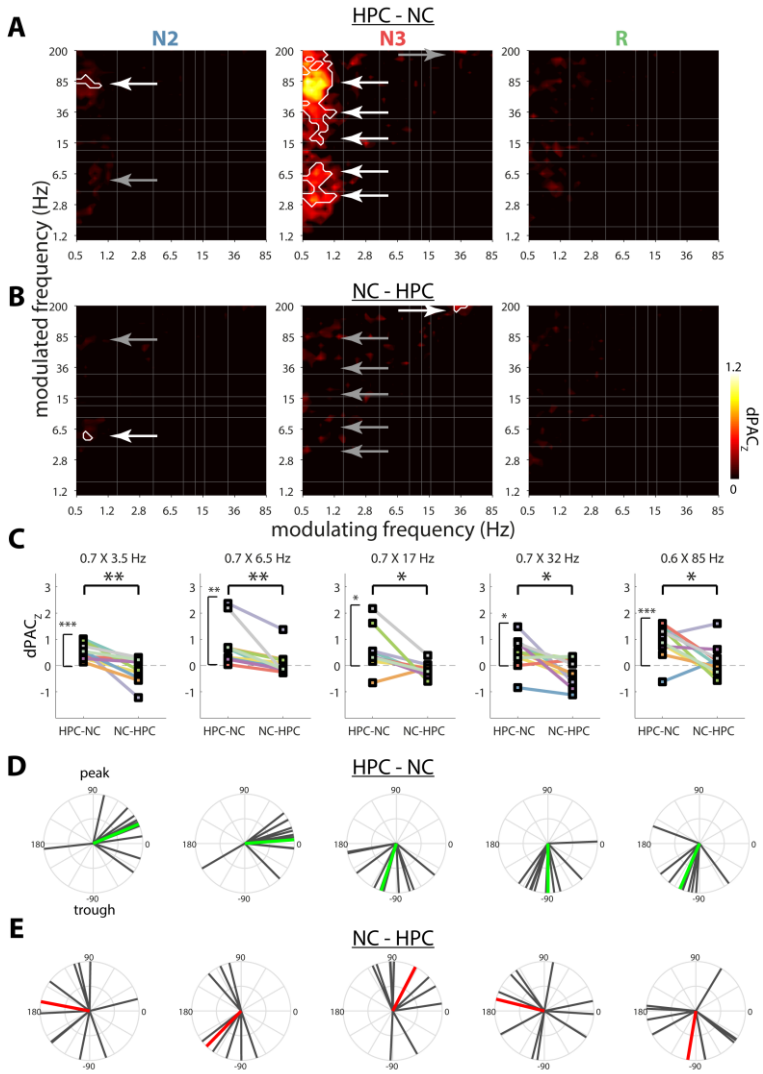

Figure 2. Cross-frequency coupling between hippocampus and neocortex. Coupling strengths for HPC-NC (A) and NC-HPC PAC (B). White outlines indicate clusters of significantly greater than zero coupling across patients (cluster-based permutation test). (C) Comparisons of HPC-NC and NC-HPC PAC for each SO-based N3 cluster (indicated in panels A and B with arrows). * P<0.05, ** P<0.01, *** P<0.001 (uncorrected). (D and E) SO phase (with respect to sine wave) at which faster activity is maximally expressed across patients for HPC-NC (D) and NC-HPC (E) PAC. Colored lines indicate group averages, with green indicating significant (P<0.05) deviations from uniformity, and red nonsignificance.

bioRxiv preprint doi: https://doi.org/10.1101/745745; this version posted August 24, 2019. The copyright holder for this preprint (which was not certified by peer review) is the author/funder, who has granted bioRxiv a license to display the preprint in perpetuity. It is made available under aCC-BY-NC 4.0 International license.

Contrary to the robust modulation of NC activity by HPC SOs, NC SOs only provided a weak though significant coordination of HPC dynamics in the theta (5.8 Hz) band during N2 ("NC-HPC PAC", Fig. 2B). No modulating influence of NC SOs was found on HPC activity during N3, but a weak N3 cluster was found for low gamma-high gamma PAC (32 x 200 Hz). Again, no interregional NC-HPC PAC was observed during REM. Of note, individual profiles of interregional coupling were consistent with these group-level findings (Supp. Fig. 7).

We further investigated the apparent asymmetries of how slower NREM frequencies coordinate distant activity in various manners. First, we extracted individuals' $dPAC_Z$ values for the 8 frequency pairs showing maximum group effects (white arrows in Fig. 2AB), along with their opposite direction counterparts (gray arrows). Unsurprisingly, coupling strength for each selected frequency pair was significantly greater than zero for the direction used for its selection (one-tailed t tests vs. zero with False Discovery Rate correction across frequency pairs: all $P_{corrected}<0.03$). In contrast, no above-chance coupling was observed in the opposite direction (all $P_{uncorrected}>0.12$). Moreover, directional comparisons indicated that interregional PAC was systematically greater for HPC-NC vs. NC-HPC coupling for the 5 SO-based frequency pairs of N3 (paired t test: all $P_{corrected}<0.05$), as further illustrated in Fig. 2C. The remaining three frequency pairs (N3: beta-high gamma; N2: SO-ripple and SO-theta) did not show directional differences in coupling (all $P_{corrected}>0.06$, but $P_{uncorrected}=0.05$ for N2 SO-theta). We also directly compared the full interregional coupling profiles of Fig. 2A and B, yielding a highly similar pattern of enhanced HPC-NC vs. NC-HPC coupling centered on the N3 SO-band (Supp. Fig. 8).

Second, we considered, for the SO-based frequency pairs of N3, the precise phase at which distant fast activity was maximally expressed. For HPC-NC PAC (Fig. 2D), phase distributions deviated substantially from uniformity for each of the five clusters (Rayleigh test for uniformity, all $P_{corrected}<0.008$), indicating that fast NC activity is preferentially expressed at similar phases of the HPC SO across patients. Specifically, delta and theta activity occurred around the negative-to-positive zero-crossing, while the spindle, low-gamma, and ripple bands showed maximal activity in the SO trough (likely reflecting the physiological up state (22)). In contrast, HPC fast activity was not consistently expressed in a particular phase range of the NC SO (all $P_{uncorrected}>0.09$, Fig. 2E), consistent with the lack of coupling reported in the previous paragraph.

Finally, we directly compared interregional HPC-NC PAC (as shown in Fig. 2A) to local PAC within each brain structure (as shown in Supp. Fig. 4AB). For both HPC and NC, cross-frequency interactions were generally stronger within than between brain structures, as shown in Fig. 3. Specifically, the phase of HPC delta (1.5-4 Hz) organized spindle/beta and ripple activity more strongly within local HPC than in distant NC for both NREM stages. This delta-ripple effect is consistent with sharp-wave-ripple complexes. Interestingly, the N3 modulation of faster activity by the HPC SO was spared from these effects of enhanced local vs. interregional PAC (red oval in Fig. 3A), suggesting that HPC SOs are equally capable of modulating faster components in local and distant brain sites. In contrast, fast NC activity in the spindle-to-high-gamma bands during N3 was coordinated more robustly by the local NC SO than the HPC SO (black arrow in Fig. 3B). These observations could indicate that while fast NC activity is under the control of HPC SOs, local SOs still exert a stronger influence. Although

bioRxiv preprint doi: https://doi.org/10.1101/745745; this version posted August 24, 2019. The copyright holder for this preprint (which was not certified by peer review) is the author/funder, who has granted bioRxiv a license to display the preprint in perpetuity. It is made available under aCC-BY-NC 4.0 International license.

some local vs. interregional differences were also seen for N2 and REM, no systematic interregional PAC was seen for these sleep stages (Fig. 2A).

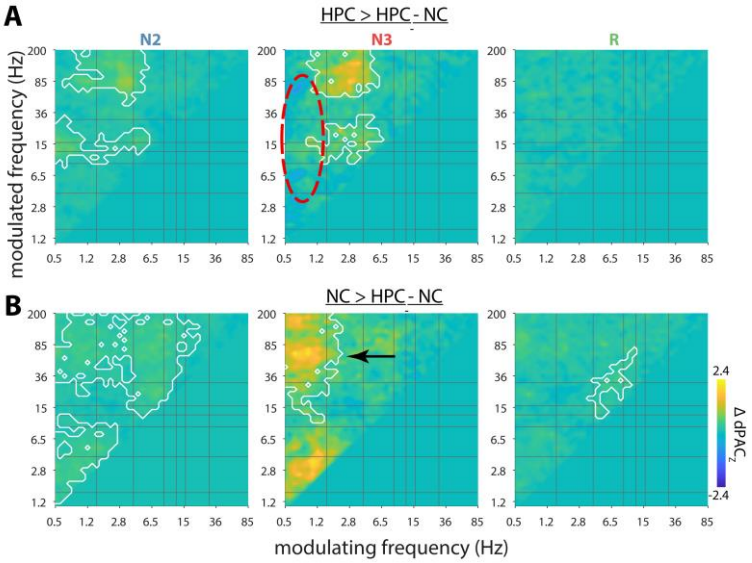

Figure 3. Differences between local and interregional cross-frequency coupling. Coupling strength differences for HPC versus HPC-NC (A) and NC versus HPC-NC (B). White outlines indicate clusters of significantly greater same-site than cross-site coupling (cluster-based permutation). No clusters with greater cross-site than same-site coupling were observed.

Overall, these findings indicate that the HPC SO phase is capable of coordinating the expression of faster activity in NC regions during N3 sleep, whereas the reverse NC-HPC modulation does not occur. Interestingly, while this modulation occurred for several distinct frequency bands, the spindle effect in particular overlaps with the frequency range showing interregional phase synchronization (Fig. 1). Hence, an intriguing possibility is that beside the local and distant modulation of faster frequencies' amplitudes, SO rhythms may also affect their interregional phase synchronization. We address this question next.

Modulation of interregional phase synchronization by hippocampal slow oscillations

As a final potential form of phase-based HPC-NC communication, we asked whether within-frequency phase synchronization for faster frequencies could vary as a function of a slower oscillatory phase. We computed HPC-NC wPLI for each modulated frequency as a function of the phase (18 bins) of each slower frequency in either HPC or NC. We then determined a modulation index (MI) (61) for each frequency pair, indicating the degree to which wPLI values are non-uniformly distributed across the cycle of a slower frequency, and further normalized MI with respect to surrogate distributions. (Due to methodological considerations related to data length, two patients were excluded from N3 analyses.)

Intriguingly, these analyses revealed a strong organizing influence from the HPC SO on interregional phase synchronization (Fig. 4A). Specifically, HPC-NC theta synchrony was reliably modulated by HPC SOs during N2, whereas spindle synchrony was coordinated by both N2 and N3 HPC SOs, similar to scalp findings (35). Note that these theta and spindle effects overlap well with the frequency bands showing interregional synchrony in Fig. 1. No other NREM effects emerged, but a small SO-beta cluster was found during REM.

bioRxiv preprint doi: https://doi.org/10.1101/745745; this version posted August 24, 2019. The copyright holder for this preprint (which was not certified by peer review) is the author/funder, who has granted bioRxiv a license to display the preprint in perpetuity. It is made available under aCC-BY-NC 4.0 International license.

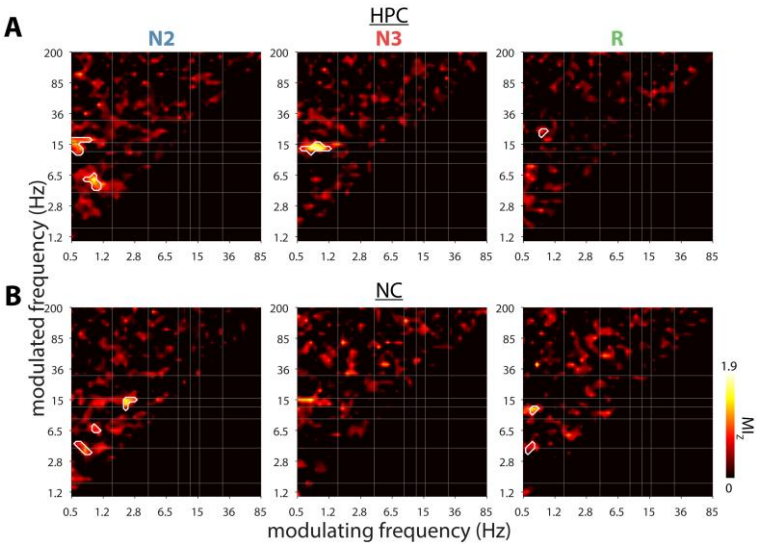

Figure 4. Cross-frequency modulation of phase synchronization between hippocampus and neocortex. Normalized modulation indices (MI_Z) for phase of HPC (A) and NC (B). White outlines indicate clusters of significantly greater than zero modulation across patients (cluster-based permutation test). N=8 for N3, N=10 for N2 and REM.

Considering how phase synchronization depends on the NC rather than HPC phase (Fig. 4B), we observed several small clusters in N2 (SO-delta, SO-theta, delta-spindle) and REM (SO-delta, SO-spindle). Again, we note the overlap with the theta and spindle phase synchronization bands of Fig. 1.

Similar to our approach for cross-regional PAC, we extracted patients MI_Z values for each of the 9 frequency pairs showing a maximal effect. Trivially, these were all significantly greater than zero (all $P_{corrected}<0.04$), whereas their counterparts in the other brain region did not differ reliably from zero (all $P_{uncorrected}>0.05$). Direct comparisons between HPC- and NC-based modulation of phase synchronization for these frequency pairs revealed a reliably greater HPC vs. NC influence of N2 SOs on theta synchrony ($P_{corrected}=0.06$). Conversely, NC phase impacted phase synchronization more strongly than HPC phase for N2 delta-spindle ($P_{corrected}=0.06$) and REM SO-spindle pairs ($P_{corrected}=0.03$). No other effects emerged (all $P_{corrected}>0.11$). We also directly compared the full HPC and NC profiles of Fig. 4, but no significant clusters emerged (Supp. Fig. 9).

In sum, the phase of SO/delta activity orchestrates interregional phase synchronization in several faster frequency bands, most prominently the theta and spindle bands. Specifically, HPC SOs have a particularly strong impact on theta synchrony, whereas NC delta activity modulates spindle connectivity. These findings establish another major form of phase-based HPC-NC coordination, potentially contributing to systems-level memory reorganization.

Discussion

Communication between the hippocampus and neocortex during sleep is considered a cornerstone of theories of memory consolidation, but exactly how these interactions are instantiated in the human brain has remained unclear. In line with the notion that oscillatory phase is critically involved in binding distant but functionally related neural populations (31),

bioRxiv preprint doi: https://doi.org/10.1101/745745; this version posted August 24, 2019. The copyright holder for this preprint (which was not certified by peer review) is the author/funder, who has granted bioRxiv a license to display the preprint in perpetuity. It is made available under aCC-BY-NC 4.0 International license.

we observed systematic i) within-frequency phase synchronization, ii) cross-frequency phase-amplitude coupling, and iii) cross-frequency modulation of within-frequency phase synchronization, thereby uncovering several previously unknown modes of interregional HPC-NC communication. A particularly prominent role emerged for HPC SOs, coordinating both the expression of, and synchronization with, faster NC activity.

Phase synchrony between hippocampus and neocortex

As a first major form of phase-based interregional communication, we observed within-frequency theta, spindle, and beta phase synchronization between HPC and NC (Fig. 1), thus reflecting precise oscillatory coordination on a cycle-by-cycle basis for these frequency bands. Consistent phase relations between brain areas affect the relative timing of neuronal spikes, thereby enabling communication and plasticity (33, 62).

Sleep spindles are closely tied to memory and plasticity (17, 18, 63), and show widespread phase synchronization in cortical networks (35). Here, we extend these observations of NREM spindle synchrony to include dynamics between HPC and lateral temporal cortex, similar to recent observations between HPC and prefrontal areas (38). Thus, the precise coordination of spindle activity across HPC and neocortical areas may offer a potential mechanism to transiently reactivate distributed memory traces, and thereby contribute to NREM-dependent memory consolidation.

Surprisingly, similar observations of HPC-NC phase synchrony were made for N2 and REM theta. These findings may offer a physiological basis for recent work demonstrating a role for NREM theta in memory consolidation (26, 27). While the reason for the differential expression of theta connectivity during N2 and N3 is unclear, these findings underscore the need to consider these sleep stages separately. In contrast, interregional HPC-NC theta synchrony during REM sleep could form a neurobiological basis for associations between REM theta and the regulation and consolidation of emotional content (28, 29). Combined with similar findings of REM theta connectivity between prefrontal and cingulate areas (64), theta rhythms appear to be coordinated across widespread brain areas. Of note, the observed REM theta synchrony contrasts with a study reporting no REM theta coherence between HPC and NC (65). However, that observation was based on only two patients, providing limited opportunities to detect effects that may not be present in all individuals, as we also observed (e.g., Supp. Fig. 3A).

Another unexpected spectral component to exhibit phase synchrony was observed in the beta band during N3. While not present in every individual (and therefore weaker at the group level), a beta effect clearly distinct from the spindle frequency could be discerned on an individual basis (Supp. Fig. 3CF). Thus, beta activity may reflect another spectral band of interest regarding sleep function.

The absence of reliable phase synchrony in other frequency bands also deserves mention. Although raw wPLI was greatest for slower rhythms (Fig. 1A), SO synchronization after surrogate-based normalization was most limited during N3 (Fig. 1B), suggesting that HPC and NC SOs show variable phase relations (25, 38). Similarly, ripple band activity was not reliably synchronized between brain structures, consistent with analogous findings of low co-occurrence of neocortical gamma events (37). However, we note that phase synchrony

bioRxiv preprint doi: https://doi.org/10.1101/745745; this version posted August 24, 2019. The copyright holder for this preprint (which was not certified by peer review) is the author/funder, who has granted bioRxiv a license to display the preprint in perpetuity. It is made available under aCC-BY-NC 4.0 International license.

profiles differed between individuals, with synchrony in SO, ripple, and other frequency bands sometimes reliably expressed on an individual basis (Supp. Fig. 3ABC).

Cross-frequency phase-amplitude coupling between hippocampus and neocortex

As a second major form of oscillatory HPC-NC coordination, we observed systematic interregional cross-frequency phase-amplitude coupling. These effects were restricted to a governing role of HPC SOs over NC activity spanning the delta, theta, spindle/beta, low gamma, and ripple ranges (Fig. 2A). The opposite pattern, whereby the phase of NC oscillations coordinates HPC activity, for either SOs or other frequencies, was not seen (Fig. 2BC). Similarly, the preferred SO phase at which faster activity was expressed was highly consistent across patients for HPC-NC, but not NC-HPC PAC (Fig. 2DE). Of note, this asymmetry is consistent with the notion of independent HPC and NC SO dynamics, as suggested by the lack of N3 SO phase synchrony.

Although our metric of interregional PAC does not contain directional information *per se*, it is widely assumed that it is the phase of the slower frequency that modulates faster activity, rather than the other way around (39, 40). While SOs and their coordination of faster activity are typically viewed as NC phenomena (Supp. Fig. 4B), similar dynamics within HPC are now well established (Supp. Fig. 4A) (22, 24, 25, 53, 66, 67). As such, our findings suggest a driving force of HPC SOs on NC activity, co-determining NC activity in various faster frequency bands. These effects may stem from surges of local activity associated with HPC up states being transmitted to post-synaptic targets and eventually reaching NC. Indeed, while faster activity was typically modulated more strongly by local than distant slower rhythms, HPC SO activity coordinated local and NC faster activity to similar extents (Fig. 3A), potentially fostering more efficient HPC-NC information exchange.

We did not observe systematic cross-regional HPC-NC PAC for modulating rhythms beyond SOs, although we did find such examples on an individual basis (e.g., HPC-NC spindle-ripple PAC, Supp. Fig. 7A, p7). This general lack of HPC-NC PAC beyond SOs is noteworthy given that many additional frequency pairs were coupled locally in HPC and NC (Supp. Fig. 4). These findings indicate that cross-regional and local PAC are at least partially dissociated, which is further supported by the observed asymmetry between HPC-NC and NC-HPC PAC. Importantly, these findings also alleviate concerns that cross-regional PAC is due to volume conduction, whereby modulating, modulated, or both signal components primarily reflect activity from the other brain site.

The lack of systematic NC-HPC PAC in our data may appear at odds with previous observations of HPC spindles and ripples coupled to NC SOs and spindles, respectively (24, 46, 51). We note, however, that we observed both of these forms of NC-HPC PAC on an individual basis (Supp. Fig. 7B; spindle-ripple for p2, SO-spindle for p7 and p9). Moreover, previous studies observing NC-HPC PAC assessed NC activity with non-invasive scalp electrodes that aggregate activity over large spatial domains, thus reflecting common signals with relatively powerful drives. In contrast, the localized NC activity we considered here constitutes only a tiny fraction of all NC activity and may therefore exert a more limited influence on HPC activity (also see relative dissociation of scalp and NC signals in Supp. Fig. 1).

bioRxiv preprint doi: https://doi.org/10.1101/745745; this version posted August 24, 2019. The copyright holder for this preprint (which was not certified by peer review) is the author/funder, who has granted bioRxiv a license to display the preprint in perpetuity. It is made available under aCC-BY-NC 4.0 International license.

More generally, a major unresolved issue concerns the directionality of HPC-NC dynamics during sleep. Our findings of HPC SOs modulating NC faster activity but not *vice versa* are most consistent with the notion of HPC to NC directionality, as suggested by classical theoretical (15) and computational (68) models. That said, empirical evidence has been mixed, pointing towards HPC-NC (56, 69), NC-HPC (22, 54, 70), or more elaborate bidirectional paths (38, 55). Hence, observed directionality likely varies with the precise electrophysiological phenomenon under consideration. Nonetheless, our observations highlight one particular aspect of interregional dynamics whereby HPC modulates NC activity.

Cross-frequency modulation of phase synchronization

The third and final form of oscillatory HPC-NC interaction we observed was the modulation of within-frequency phase synchronization by the phase of slower rhythms. Most prominently, the HPC SO phase had a robust influence on the degree of N2 theta and NREM spindle synchrony (Fig. 4A), matching the sleep stages where these forms of synchrony were apparent (Fig. 1).

The gating of spindle synchrony by HPC SOs is highly consistent with similar observations of SO-modulated spindle synchrony in scalp data (35), and compatible with findings of enhanced HPC-prefrontal spindle synchrony for spindles coupled vs. uncoupled to frontal SOs (38). While we did not see clear evidence that NC SOs impose a similar modulation on spindle synchrony, modulation strengths also did not differ reliably between HPC and NC. On the other hand, we did observe a modulation of spindle synchrony by the NC delta phase in N2, which, furthermore, was stronger in NC than HPC. Furthermore, an SO-spindle effect that was stronger for NC than HPC was found during REM, consistent with the presence of REM SOs (48, 59, 71). Hence, strong conclusions regarding whether HPC or NC SOs most effectively affect spindle synchrony are presently not warranted.

In stark contrast, N2 theta synchrony depended to a greater extent on HPC than NC SOs. Intriguingly, this effect appears to be separate from the enhanced HPC-NC vs. NC-HPC modulation of theta amplitude by SOs, which occurred in N3 rather than N2. While the reason for this dissociation is unclear, both effects are in agreement that interregional theta dynamics are modulated most effectively by HPC rather than NC SOs.

Limitations and caveats

Although generalizing from epileptic to healthy populations poses a risk, sleep architecture (Supp. Table 1) was in line with healthy sleep. Moreover, we employed a rigorous artifact rejection protocol, and only considered electrodes on the non-pathological side, making it unlikely our results are due to epileptogenic activity. In the present approach, measures of oscillatory coordination were calculated over continuous data. This contrasts with discrete approaches where analyses are contingent on the presence of specific waveforms. Given that our approach identified various expected phenomena of local PAC (e.g., SO-spindle, spindle-ripple), we do not believe this methodological choice poses a major concern. That said, future work may scrutinize individual waveforms to fully understand the origin of each of the observed effects (72).

We examined communication between HPC and lateral temporal cortex, a neocortical region that has not received much attention in the context of sleep-dependent memory

bioRxiv preprint doi: https://doi.org/10.1101/745745; this version posted August 24, 2019. The copyright holder for this preprint (which was not certified by peer review) is the author/funder, who has granted bioRxiv a license to display the preprint in perpetuity. It is made available under aCC-BY-NC 4.0 International license.

consolidation. Although precise electrode placement varied across patients (Supp. Table 2), the role of lateral temporal cortex in long-term memory storage (8, 9) makes it well-suited for studying HPC-NC interactions. Future work should address whether the reported forms of phase coordination apply more broadly to other NC sites.

Conclusion

The present observations of coupled HPC-NC sleep oscillations further cement the fundamental role of precisely coordinated oscillatory rhythms in neural communication (30–32). As such, they establish an important prerequisite for memory consolidation theories postulating a sleep-dependent HPC-NC dialog (2, 13, 14). More specifically, the identified forms of phase coordination draw attention not only to SOs and spindles, but also to theta and beta activity. Similarly, the asymmetrical coordination of NC activity by HPC SOs suggests that HPC may play a larger orchestrating role in information exchange during sleep than previously thought. Overall, these findings refine our knowledge of human HPC-NC interactions and offer novel opportunities to understand the determinants of sleep-dependent memory consolidation in health and disease.

Methods

Participants

We analyzed archival electrophysiological sleep data in a sample of 10 (6 male) patients suffering from pharmaco-resistant epilepsy (age: 36.6 ± 14.8 yrs, range: 22–62). This sample overlaps with ones presented previously (24, 48, 54). Aspects of the HPC data were recently described in detail elsewhere (48), but are summarily included here both because of different patient and electrode inclusion criteria and to provide a comprehensive perspective on HPC-NC oscillations. Patients had been epileptic for 22.5 ± 11.0 yrs (range: 10–49) and were receiving anticonvulsive medication at the moment of recording. All patients gave informed consent, the study was conducted according to the Declaration of Helsinki, and was approved by the ethics committee of the Medical Faculty of the University of Bonn.

Data acquisition

Electrophysiological monitoring was performed with a combination of depth and subdural strip/grid electrodes. HPC depth electrodes (AD-Tech, Racine, WI, USA) containing 8–10 cylindrical platinum-iridium contacts (length: 1.6 mm; diameter: 1.3 mm; center-to-center inter-contact distance: 4.5 mm) were stereotactically implanted. Implantations were done either bilaterally (n=7) or unilaterally (n=3), and either along the longitudinal HPC axis via the occipital lobe (n=9) or along a medial-lateral axis via temporal cortex (n=1). Stainless steel subdural strip/grid electrodes were of variable size with contact diameters of 4 mm and center-to-center spacing of 10 mm, and placed over various cortical areas according to clinical criteria. Anatomical labels of each electrode were determined based on pre- and post-implantation magnetic resonance image (MRI) scans by an experienced physician (TR), as described previously (48).

A single grey matter HPC electrode and a single NC electrode from lateral temporal cortex were selected for each patient. As reported previously for HPC, and here additionally seen for NC, within-patient spectral profiles varied between adjacent contacts. Following previous approaches (24) and the hypothesized central role of spindles in HPC-NC communication, at both brain sites the contact with highest NREM spindle power was chosen.

bioRxiv preprint doi: https://doi.org/10.1101/745745; this version posted August 24, 2019. The copyright holder for this preprint (which was not certified by peer review) is the author/funder, who has granted bioRxiv a license to display the preprint in perpetuity. It is made available under aCC-BY-NC 4.0 International license.

Electrode locations for each patient are indicated in Table 1. For HPC, fast spindle peaks were visible for all patients. For NC, 7 of 10 patients showed fast spindle peaks, one showed a slow spindle peak, and two did not exhibit noticeable spindle peaks. Additional non-invasive signals were recorded from the scalp (Cz, C3, C4, Oz, A1, A2; plus T5 and T6 in 8 patients), the outer canthi of the eyes for electrooculography (EOG), and chin for electromyography (EMG). All signals were sampled at 1 kHz (Stellate GmbH, Munich, Germany) with hardware low- and high-pass filters at 0.01 and 300 Hz respectively, using an average-mastoid reference. Offline sleep scoring was done in 20 s epochs based on scalp EEG, EOG, and EMG signals in accordance with Rechtschaffen and Kales criteria (73). Stages S3 and S4 were combined into a single N3 stage following the more recent criteria of the American Academy of Sleep Medicine (74).

Preprocessing and artifact rejection

All data processing and analysis was performed in Matlab (the Mathworks, Natick, MA), using custom routines and EEGLAB functionality (75). Preprocessing and artifact rejection details are identical to our previous report (48). Briefly, data were high-pass (0.3 Hz) and notch (50 Hz and harmonics up to 300 Hz) filtered, and channel-specific thresholds (z-score > 6) of signal gradient and high-frequency (>250 Hz) activity were applied to detect and exclude epileptogenic activity. Artifact-free data "trials" of at least 3 s were kept for subsequent processing, resulting in a total of 78.1 ± 30.8 (N2), 21.7 ± 17.8 (N3), and 44.5 ± 23.7 min (REM) of usable data.

Time-frequency decomposition

Data were decomposed with a family of complex Morlet wavelets. Each trial was extended with 5 s on either side to minimize edge artifacts. Wavelets were defined in terms of desired temporal resolution according to:

$$wavelet = e^{i2\pi tf} * e^{-4\ln(2)t^2/h^2} \quad (1)$$

where i is the imaginary operator, t is time in seconds, f is frequency (50 logarithmically spaced frequencies between 0.5 and 200 Hz), ln is the natural logarithm, and h is temporal resolution (full-width at half-maximum; FWHM) in seconds (76). We set h to be logarithmically spaced between 3 s (at 0.5 Hz) and 0.025 s (at 200 Hz), resulting in FWHM spectral resolutions of 0.3 and 35 Hz, respectively. Trial padding was trimmed from the convolution result, which was subsequently downsampled by a factor four to reduce the amount of data. We normalized phase-based metrics using surrogate approaches (see below). To make surrogate distributions independent of variable numbers and durations of trials, we first concatenated the convolution result of all trials of a given sleep stage, and then segmented them into 60 s fragments (discarding the final, incomplete segment).

Phase synchrony

To assess within-frequency phase synchrony, we used the weighted phase lag index (wPLI) (57), a measure of phase synchrony that de-weights zero phase (and antiphase) connectivity. For every 60 s segment and frequency band, raw wPLI between seed channel j (HPC) and target channel k (NC) was calculated as:

bioRxiv preprint doi: https://doi.org/10.1101/745745; this version posted August 24, 2019. The copyright holder for this preprint (which was not certified by peer review) is the author/funder, who has granted bioRxiv a license to display the preprint in perpetuity. It is made available under aCC-BY-NC 4.0 International license.

$$wPLI_{jk} = \frac{\left|\frac{1}{n}\sum_{t=1}^{n}|imag(S_{jkt})|sgn\left(imag(S_{jkt})\right)\right|}{\frac{1}{n}\sum_{t=1}^{n}|imag(S_{jkt})|} \quad (2)$$

where *imag* indicates the imaginary part, S_{jkt} is the cross-spectral density between signals *j* and *k* at sample *t*, and *sgn* indicates the sign. We further created a normalized version of this metric using a surrogate approach. Surrogates were constructed by repeatedly (n = 100) time shifting the phase time series of the seed channel by a random amount between 1 and 59 s, and recalculating wPLI for each iteration. Note that time shifting is a more conservative approach than fully scrambling time series, which may result in spurious effects (77). This distribution was then used to z-score the raw wPLI value. Thus, the z-scored measure ($wPLI_Z$) indicates how far, in terms of standard deviations, the observed coupling estimate is removed from the average coupling estimate under the null hypothesis of no coupling. We used the median to further aggregate wPLI and $wPLI_Z$ values across data segments.

Cross-frequency phase-amplitude coupling

For every 60 s segment, PAC was determined between all pairs of modulating frequency *f1* and modulated frequency *f2*, where *f2*>2**f1*. We employed an adaptation of the mean vector length method (78) that adjusts for possible bias stemming from non-sinusoidal shapes of *f1* (60). Specifically, complex-valued debiased phase-amplitude coupling (dPAC) was calculated as:

$$\text{dPAC} = \frac{1}{n}\sum_{t=1}^{n}(amp_{f2}(t) * (e^{i\varphi_{f1}(t)} - B)) \quad (3)$$

where *i* is the imaginary operator, *t* is time, $amp_{f2}(t)$ is the magnitude of the convolution result, or amplitude, of *f2*, $\varphi_{f1}(t)$ is the phase of *f1*, and *B* is the mean phase bias:

$$B = \frac{1}{n}\sum_{t=1}^{n} e^{i\varphi_{f1}(t)} \quad (4)$$

For same-site PAC (i.e., within HPC or within NC) φ_{f1} and amp_{f2} stemmed from the same electrode, whereas cross-site PAC used phase information from one brain structure and amplitude information from the other. Raw coupling strength (i.e., the degree to which the *f2* amplitude is non-uniformly distributed over *f1* phases) was defined as the magnitude (i.e., length) of the mean complex vector. For every 60 s segment, frequency pair, and same/cross-site combination we constructed a surrogate distribution of coupling strengths by repeatedly (n = 100) time shifting the *f1* phase time series with respect to the *f2* amplitude time series, and recalculating the mean vector length for each iteration. We then z-scored the observed coupling strength with respect to this null distribution of coupling strength values. We used the median to further aggregate $dPAC_Z$ values across data segments.

Cross-frequency modulation of phase synchrony

A modulation index (MI) was computed between all pairs of modulating frequency *f1* and modulated frequency *f2*, where *f2*>2**f1*. For each frequency *f1*, samples were binned according to phase φ_{f1} (18 bins), and wPLI was calculated for each bin *b* and frequency *f2* following equation (2). Segment-averaged wPLI values were then used to calculate raw MI as:

bioRxiv preprint doi: https://doi.org/10.1101/745745; this version posted August 24, 2019. The copyright holder for this preprint (which was not certified by peer review) is the author/funder, who has granted bioRxiv a license to display the preprint in perpetuity. It is made available under aCC-BY-NC 4.0 International license.

$$\mathrm{MI} = \left|\frac{1}{n}\sum_{b=1}^{n}(wPLI_{f2}(b) * (e^{i\varphi_b}))\right| \quad (5)$$

where *b* is the bin number, *n* is the number of bins (18), and φ_b is the phase at each bin center. This calculation was performed separately for HPC and NC *f1* phases. Note that MI was calculated across all available segments rather than per 60 s segment (as for wPLI and dPAC) because segment-wise MI estimates proved unstable. Similarly, surrogate distributions were constructed by repeatedly (n=100) shuffling the pairing of *f1* and *f2* phase segments (disallowing pairings where individual segments were unaltered), and recalculating MI across segments for each iteration, rather than per segment. Since the number of unique segment pairings depends on the number of available segments, 2 patients were excluded from N3 analyses. Observed MI values were z-scored with respect to their null distributions to generate normalized MI_Z.

Statistics

Statistical analyses were performed at both the group (wPLI, dPAC, MI) and individual (wPLI, dPAC) levels using cluster-based permutation tests (79) with a *clusteralpha* value of 0.1. We used 1000 random permutations for most tests (i.e., N≥10), except for several cases where the number of possible permutations was lower (when N≤9), in which case each unique permutation was used exactly once. To determine the presence of effects, $wPLI_Z$, $dPAC_Z$, and MI_Z values at each frequency/frequency pair were compared to zero across patients (group) or data segments (individual) with one-tailed tests. Comparisons between sleep stages, regions, and directions were performed with two-tailed paired tests. Clusters were deemed significant at $P<0.05$ (one-tailed) and $P<0.025$ (two-tailed). For $dPAC_Z$ and MI_Z, clusters were required to span at least 2 x 2 frequency bins.

Data and code availability

Data are not publicly available due to privacy concerns related to clinical data, but data and accompanying analysis code are available from the corresponding or senior author upon obtaining ethical approval.

Acknowledgments

This work was supported by the German Research Foundation (FE366/9-1 to JF) and a Wellcome Trust/Royal Society Sir Henry Dale Fellowship (107672/Z/15/Z to BPS).

References

1. Marr D (1971) Simple memory: a theory for archicortex. *Philos Trans R Soc Lond B Biol Sci* 262(841):23–81.

2. Buzsáki G (1996) The Hippocampo-Neocortical Dialogue. *Cereb Cortex* 6(2):81–92.

3. Frankland PW, Bontempi B (2005) The organization of recent and remote memories. *Nat Rev Neurosci* 6(2):119–130.

4. Scoville WB, Milner B (1957) Loss of recent memory after bilateral hippocampal lesions. *J Neurol Neurosurg Psychiatry* 20(1):11–21.

5. Zola-Morgan S, Squire L (1990) The primate hippocampal formation: evidence for a time-limited role in memory storage. *Science* 250(4978):288–290.

bioRxiv preprint doi: https://doi.org/10.1101/745745; this version posted August 24, 2019. The copyright holder for this preprint (which was not certified by peer review) is the author/funder, who has granted bioRxiv a license to display the preprint in perpetuity. It is made available under aCC-BY-NC 4.0 International license.

6. Takashima A, et al. (2009) Shift from Hippocampal to Neocortical Centered Retrieval Network with Consolidation. *J Neurosci* 29(32):10087–10093.

7. Bonnici HM, et al. (2012) Detecting Representations of Recent and Remote Autobiographical Memories in vmPFC and Hippocampus. *J Neurosci* 32(47):16982–16991.

8. Graham KS, Hodges JR (1997) Differentiating the roles of the hippocampal complex and the neocortex in long-term memory storage: evidence from the study of semantic dementia and Alzheimer's disease. *Neuropsychology* 11(1):77–89.

9. Bayley PJ, Gold JJ, Hopkins RO, Squire LR (2005) The Neuroanatomy of Remote Memory. *Neuron* 46(5):799–810.

10. Baylis G, Rolls E, Leonard C (1987) Functional subdivisions of the temporal lobe neocortex. *J Neurosci* 7(2):330–342.

11. Kriegeskorte N, Formisano E, Sorger B, Goebel R (2007) Individual faces elicit distinct response patterns in human anterior temporal cortex. *Proc Natl Acad Sci* 104(51):20600–20605.

12. Zahn R, et al. (2007) Social concepts are represented in the superior anterior temporal cortex. *Proc Natl Acad Sci* 104(15):6430–6435.

13. Rasch B, Born J (2013) About Sleep's Role in Memory. *Physiol Rev* 93(2):681–766.

14. Stickgold R, Walker MP (2013) Sleep-dependent memory triage: evolving generalization through selective processing. *Nat Neurosci* 16(2):139–145.

15. Buzsáki G (1998) Memory consolidation during sleep: a neurophysiological perspective. *J Sleep Res* 7(S1):17–23.

16. Axmacher N, Elger CE, Fell J (2008) Ripples in the medial temporal lobe are relevant for human memory consolidation. *Brain* 131(7):1806–1817.

17. Cairney SA, Guttesen A á V, El Marj N, Staresina BP (2018) Memory Consolidation Is Linked to Spindle-Mediated Information Processing during Sleep. *Curr Biol* 28(6):948-954.e4.

18. Cox R, Hofman WF, de Boer M, Talamini LM (2014) Local sleep spindle modulations in relation to specific memory cues. *NeuroImage* 99:103–110.

19. Huber R, Ghilardi MF, Massimini M, Tononi G (2004) Local sleep and learning. *Nature* 430(6995):78–81.

20. Schönauer M, et al. (2017) Decoding material-specific memory reprocessing during sleep in humans. *Nat Commun* 8:15404.

21. Zhang H, Fell J, Axmacher N (2018) Electrophysiological mechanisms of human memory consolidation. *Nat Commun* 9(1). doi:10.1038/s41467-018-06553-y.

22. Nir Y, et al. (2011) Regional Slow Waves and Spindles in Human Sleep. *Neuron* 70(1):153–169.

23. Andrillon T, et al. (2011) Sleep Spindles in Humans: Insights from Intracranial EEG and Unit Recordings. *J Neurosci* 31(49):17821–17834.

bioRxiv preprint doi: https://doi.org/10.1101/745745; this version posted August 24, 2019. The copyright holder for this preprint (which was not certified by peer review) is the author/funder, who has granted bioRxiv a license to display the preprint in perpetuity. It is made available under aCC-BY-NC 4.0 International license.

24. Staresina BP, et al. (2015) Hierarchical nesting of slow oscillations, spindles and ripples in the human hippocampus during sleep. *Nat Neurosci* 18(11):1679–1686.

25. Wolansky T, Clement EA, Peters SR, Palczak MA, Dickson CT (2006) Hippocampal Slow Oscillation: A Novel EEG State and Its Coordination with Ongoing Neocortical Activity. *J Neurosci* 26(23):6213–6229.

26. Schreiner T, Lehmann M, Rasch B (2015) Auditory feedback blocks memory benefits of cueing during sleep. *Nat Commun* 6(1). doi:10.1038/ncomms9729.

27. Schreiner T, Doeller CF, Jensen O, Rasch B, Staudigl T (2018) Theta phase coordinated memory reactivation reoccurs in a slow-oscillatory rhythm during NREM sleep. *Cell Rep* 25:296–301.

28. Nishida M, Pearsall J, Buckner RL, Walker MP (2009) REM Sleep, Prefrontal Theta, and the Consolidation of Human Emotional Memory. *Cereb Cortex* 19(5):1158–1166.

29. Sopp MR, Brueckner AH, Schäfer SK, Lass-Hennemann J, Michael T (2019) REM theta activity predicts re-experiencing symptoms after exposure to a traumatic film. *Sleep Med* 54:142–152.

30. Jacobs J, Kahana MJ, Ekstrom AD, Fried I (2007) Brain Oscillations Control Timing of Single-Neuron Activity in Humans. *J Neurosci* 27(14):3839–3844.

31. Sauseng P, Klimesch W (2008) What does phase information of oscillatory brain activity tell us about cognitive processes? *Neurosci Biobehav Rev* 32(5):1001–1013.

32. Thut G, Miniussi C, Gross J (2012) The Functional Importance of Rhythmic Activity in the Brain. *Curr Biol* 22(16):R658–R663.

33. Fell J, Axmacher N (2011) The role of phase synchronization in memory processes. *Nat Rev Neurosci* 12(2):105–118.

34. Mezeiová K, Paluš M (2012) Comparison of coherence and phase synchronization of the human sleep electroencephalogram. *Clin Neurophysiol* 123(9):1821–1830.

35. Cox R, van Driel J, de Boer M, Talamini LM (2014) Slow Oscillations during Sleep Coordinate Interregional Communication in Cortical Networks. *J Neurosci* 34(50):16890–16901.

36. Zerouali Y, et al. (2014) A time-frequency analysis of the dynamics of cortical networks of sleep spindles from MEG-EEG recordings. *Front Neurosci* 8:310.

37. Valderrama M, et al. (2012) Human Gamma Oscillations during Slow Wave Sleep. *PLoS ONE* 7(4):e33477.

38. Helfrich RF, et al. (2019) Bidirectional prefrontal-hippocampal dynamics organize information transfer during sleep in humans. *Nat Commun* 10(1). doi:10.1038/s41467-019-11444-x.

39. Aru J, et al. (2015) Untangling cross-frequency coupling in neuroscience. *Curr Opin Neurobiol* 31:51–61.

40. Canolty RT, Knight RT (2010) The functional role of cross-frequency coupling. *Trends Cogn Sci* 14(11):506–515.

bioRxiv preprint doi: https://doi.org/10.1101/745745; this version posted August 24, 2019. The copyright holder for this preprint (which was not certified by peer review) is the author/funder, who has granted bioRxiv a license to display the preprint in perpetuity. It is made available under aCC-BY-NC 4.0 International license.

41. Cox R, Mylonas DS, Manoach DS, Stickgold R (2018) Large-Scale Structure and Individual Fingerprints of Locally Coupled Sleep Oscillations. *Sleep*. doi:10.1093/sleep/zsy175.

42. Mak-McCully RA, et al. (2017) Coordination of cortical and thalamic activity during non-REM sleep in humans. *Nat Commun* 8:15499.

43. Mölle M, Bergmann TO, Marshall L, Born J (2011) Fast and Slow Spindles during the Sleep Slow Oscillation: Disparate Coalescence and Engagement in Memory Processing. *Sleep* 34(10):1411–1421.

44. Klinzing JG, et al. (2016) Spindle activity phase-locked to sleep slow oscillations. *NeuroImage* 134:607–616.

45. Clemens Z, et al. (2007) Temporal coupling of parahippocampal ripples, sleep spindles and slow oscillations in humans. *Brain* 130(11):2868–2878.

46. Clemens Z, et al. (2011) Fine-tuned coupling between human parahippocampal ripples and sleep spindles: Ripple-spindle events in human sleep. *Eur J Neurosci* 33(3):511–520.

47. Born J, Rasch B, Gais S (2006) Sleep to Remember. *The Neuroscientist* 12(5):410–424.

48. Cox R, Rüber T, Staresina BP, Fell J (2019) Heterogeneous profiles of coupled sleep oscillations in human hippocampus. *bioRxiv*. doi:10.1101/589978.

49. Steriade M, Nuñez A, Amzica F (1993) Intracellular analysis of relations between the slow (< 1 Hz) neocortical oscillation and other sleep rhythms of the electroencephalogram. *J Neurosci* 13(8):3266–3283.

50. Gonzalez CE, et al. (2018) Theta bursts precede, and spindles follow, cortical and thalamic downstates in human NREM sleep. *J Neurosci* 38:9989 –10001.

51. Latchoumane C-FV, Ngo H-VV, Born J, Shin H-S (2017) Thalamic Spindles Promote Memory Formation during Sleep through Triple Phase-Locking of Cortical, Thalamic, and Hippocampal Rhythms. *Neuron* 95(2):424-435.e6.

52. Bergmann TO, Staresina BP (2017) Neuronal Oscillations and Reactivation Subserving Memory Consolidation. *Cognitive Neuroscience of Memory Consolidation*, eds Axmacher N, Rasch B (Springer International Publishing, Cham), pp 185–207.

53. Dickson CT (2010) Ups and downs in the hippocampus: The influence of oscillatory sleep states on “neuroplasticity” at different time scales. *Behav Brain Res* 214(1):35–41.

54. Wagner T, Axmacher N, Lehnertz K, Elger CE, Fell J (2010) Sleep-dependent directional coupling between human neocortex and hippocampus. *Cortex* 46(2):256–263.

55. Rothschild G, Eban E, Frank LM (2017) A cortical–hippocampal–cortical loop of information processing during memory consolidation. *Nat Neurosci* 20(2):251–259.

56. Maingret N, Girardeau G, Todorova R, Goutierre M, Zugaro M (2016) Hippocampo-cortical coupling mediates memory consolidation during sleep. *Nat Neurosci* 19(7):959–964.

bioRxiv preprint doi: https://doi.org/10.1101/745745; this version posted August 24, 2019. The copyright holder for this preprint (which was not certified by peer review) is the author/funder, who has granted bioRxiv a license to display the preprint in perpetuity. It is made available under aCC-BY-NC 4.0 International license.

57. Vinck M, Oostenveld R, Van Wingerden M, Battaglia F, Pennartz CMA (2011) An improved index of phase-synchronization for electrophysiological data in the presence of volume-conduction, noise and sample-size bias. *NeuroImage* 55(4):1548–1565.

58. Arnulfo G, Hirvonen J, Nobili L, Palva S, Palva JM (2015) Phase and amplitude correlations in resting-state activity in human stereotactical EEG recordings. *NeuroImage* 112:114–127.

59. Funk CM, Honjoh S, Rodriguez AV, Cirelli C, Tononi G (2016) Local Slow Waves in Superficial Layers of Primary Cortical Areas during REM Sleep. *Curr Biol* 26(3):396–403.

60. van Driel J, Cox R, Cohen MX (2015) Phase-clustering bias in phase–amplitude cross-frequency coupling and its removal. *J Neurosci Methods* 254:60–72.

61. Tort ABL, Komorowski R, Eichenbaum H, Kopell N (2010) Measuring Phase-Amplitude Coupling Between Neuronal Oscillations of Different Frequencies. *J Neurophysiol* 104(2):1195–1210.

62. Fries P (2005) A mechanism for cognitive dynamics: neuronal communication through neuronal coherence. *Trends Cogn Sci* 9(10):474–480.

63. Rosanova M, Ulrich D (2005) Pattern-specific associative long-term potentiation induced by a sleep spindle-related spike train. *J Neurosci* 25(41):9398–9405.

64. Vijayan S, Lepage KQ, Kopell NJ, Cash SS (2017) Frontal beta-theta network during REM sleep. *eLife* 6. doi:10.7554/eLife.18894.

65. Cantero JL, et al. (2003) Sleep-Dependent Theta Oscillations in the Human Hippocampus and Neocortex. *J Neurosci*:7.

66. Schall KP, Kerber J, Dickson CT (2008) Rhythmic Constraints on Hippocampal Processing: State and Phase-Related Fluctuations of Synaptic Excitability During Theta and the Slow Oscillation. *J Neurophysiol* 99(2):888–899.

67. Schall KP, Dickson CT (2009) Changes in hippocampal excitatory synaptic transmission during cholinergically induced theta and slow oscillation states. *Hippocampus* 20(2):279–292.

68. McClelland JL, McNaughton BL, O'Reilly RC (1995) Why there are complementary learning systems in the hippocampus and neocortex: insights from the successes and failures of connectionist models of learning and memory. *Psychol Rev* 102(3):419–457.

69. Peyrache A, Khamassi M, Benchenane K, Wiener SI, Battaglia FP (2009) Replay of rule-learning related neural patterns in the prefrontal cortex during sleep. *Nat Neurosci* 12(7):919–926.

70. Sirota A, Csicsvari J, Buhl D, Buzsáki G (2003) Communication between neocortex and hippocampus during sleep in rodents. *Proc Natl Acad Sci* 100(4):2065–2069.

71. Bódizs R, et al. (2001) Rhythmic hippocampal slow oscillation characterizes REM sleep in humans: Hippocampal RSA in Human REM Sleep. *Hippocampus* 11(6):747–753.

72. Cole SR, Voytek B (2017) Brain Oscillations and the Importance of Waveform Shape. *Trends Cogn Sci* 21(2):137–149.

73. Rechtschaffen A, Kales A (1968) *A Manual of Standardized Terminology, Techniques and Scoring System for Sleep Stages of Human Subjects*.

bioRxiv preprint doi: https://doi.org/10.1101/745745; this version posted August 24, 2019. The copyright holder for this preprint (which was not certified by peer review) is the author/funder, who has granted bioRxiv a license to display the preprint in perpetuity. It is made available under aCC-BY-NC 4.0 International license.

74. Silber MH, et al. (2007) The visual scoring of sleep in adults. *J Clin Sleep Med* 3(2):121–131.

75. Delorme A, Makeig S (2004) EEGLAB: an open source toolbox for analysis of single-trial EEG dynamics including independent component analysis. *J Neurosci Methods* 134(1):9–21.

76. Cohen MX (2019) A better way to define and describe Morlet wavelets for time-frequency analysis. *NeuroImage* 199:81–86.

77. Scheffer-Teixeira R, Tort AB (2016) On cross-frequency phase-phase coupling between theta and gamma oscillations in the hippocampus. *eLife* 5. doi:10.7554/eLife.20515.

78. Canolty RT, et al. (2006) High gamma power is phase-locked to theta oscillations in human neocortex. *Science* 313(September):1626–1628.

79. Maris E, Oostenveld R (2007) Nonparametric statistical testing of EEG- and MEG-data. *J Neurosci Methods* 164(1):177–190.